NATIONAL ADVISORY COMMITTEE FOR AERONAUTICS

TECHNICAL NOTE

No. 1768

A RAPID GRAPHICAL METHOD FOR COMPUTING THE PRESSURE DISTRIBUTION AT SUPERSONIC SPEEDS ON A SLENDER ARBITRARY BODY OF REVOLUTION

By Jim Rogers Thompson

Langley Aeronautical Laboratory
Langley Field, Va.

Washington

January 1949

NATIONAL ADVISORY COMMITTEE FOR AERONAUTICS

TECHNICAL NOTE NO. 1768

A RAPID GRAPHICAL METHOD FOR COMPUTING THE PRESSURE DISTRIBUTION AT SUPERSONIC SPEEDS ON A SLENDER ARBITRARY BODY OF REVOLUTION

By Jim Rogers Thompson

SUMMARY

A method is presented by which the pressure distribution on a slender, arbitrary body of revolution moving at supersonic speeds at zero angle of attack may be calculated with an appreciable saving of time as compared with that required by other methods. The method was developed from the linearized potential-flow relations given by Jones and Margolis in NACA TN No. 1081 and is essentially a graphical computing technique based on the assumption that a body may be represented satisfactorily by a relatively small number of point sources and sinks. An example is presented to illustrate the computational procedure.

The method gives results for parabolic bodies in excellent agreement with results obtained by the method of Jones and Margolis. It was found that a parabolic body of fineness ratio 6 could be represented satisfactorily by as few as 10 sources and sinks.

Pressure distributions computed for the German missile A4V1P at Mach numbers of 1.87 and 1.56 are compared with wind-tunnel measurements and with results of calculations by the characteristics methods of Sauer and Tollmein to provide some information on the accuracy and reliability of the method presented herein when applied to arbitrary shapes. Although the body of the A4V1P is somewhat more blunt than would be desirable for treatment by linearized methods, the method presented reproduces the salient features of the measured pressure distribution with comparatively small discrepancies.

INTRODUCTION

The problem of computing the pressure distribution on a body of revolution moving at supersonic speeds has been treated by several authors (references 1 to 6) with varying degrees of approximation. References 1 to 5 present methods based on the isentropic linearized potential-flow equation first applied to the problem by Von Kármán in reference 1. A more rigorous method based on the method of characteristics is also presented in reference 5 and is generalized by Ferri in reference 6 to include nonisentropic rotational flows. The usefulness

of these methods for the design of supersonic aircraft or missiles has been severely limited, however, by the excessive labor involved in the computations.

Jones and Margolis (reference 4) and Lighthill (reference 3) have shown that, for certain mathematical body shapes, the pressure distribution may be obtained in the form of relatively simple equations. In general, however, the designer cannot utilize these simple mathematical shapes exclusively because of other requirements of the design; for example, providing vision for the pilot or seeker, tankage space equally distributed about the center of gravity, and shape changes to allow simpler or stronger construction. In addition, the possibility exists that body shapes other than those specified by simple mathematical relations might have the lowest drag, particularly when these shapes are combined with wings to form a practical airplane or missile configuration. The need of a rapid method for computing the pressure distribution on arbitrary bodies is therefore evident.

An approximate method for computing the pressure distribution on slender, arbitrary bodies of revolution moving at supersonic speeds and zero angle of attack is presented herein. Use of a graphical computing technique allows the pressure distribution to be obtained at an appreciable saving in time as compared with other methods. The method (which is referred to hereinafter as the "point-source method") was developed from the results of Jones and Margolis (reference 4) and is based on a simplifying assumption concerning the source distribution used to represent the body. The validity of this assumption in the case of parabolic bodies is examined by comparison of results obtained by the point-source method with results obtained by the method of Jones and Margolis.

Although results obtained by the point-source method are subject to the uncertainties inherent in the linearized potential-flow equations and to additional uncertainties due to the graphical approximations used in the computations, the method is believed to provide a quick and useful means for comparing the supersonic characteristics of slender, arbitrary bodies of revolution. Some information concerning the reliability of the results was obtained by comparison of pressure distributions computed by the point-source method with calculations by the characteristics method and with wind-tunnel measurements presented in references 7 and 8 for the German missile A4V1P.

The computational procedure for the point-source method is illustrated by an example.

SYMBOLS

P	pressure coefficient
x,r	cylindrical coordinates

ξ	abscissa of source or sink (measured along x-axis)
$f'(\xi)$	rate of change of source strength (with x)
R	radius of body
F	fineness ratio of body
θ	half angle of cone
Q	pressure function ($f'(\xi)\Delta x$)
Δx	interval length
n	positive integer
k	constant
M	Mach number

$\beta = \sqrt{M^2 - 1}$

Subscripts indicate that the value of the quantity being considered is taken at that particular point. Subscript o refers to the nose of the body.

DEVELOPMENT OF METHOD

In reference 4 Jones and Margolis show that a slender body of revolution moving at supersonic speed with zero angle of attack may be approximated by an infinite number of sources or sinks located on the axis of the body and that the pressure coefficient P at any point x on the body surface is given by

$$P_x = 2 \int_{x_o}^{x-\beta R_x} \frac{f'(\xi)\, d\xi}{\sqrt{(x-\xi)^2 - (\beta R_x)^2}} \tag{1}$$

where $f'(\xi)$ is the first derivative of the function

$$f(\xi) = \left[R\left(\frac{dR}{dx}\right)\right]_\xi \tag{2}$$

Explicit relations may be easily obtained from equations (1) and (2) for the pressure distribution on cones and on parabolic bodies. For arbitrary

bodies, the pressure distribution can also be computed directly from equations (1) and (2) (provided that $f(\xi)$ is a continuous function of x) by either analytical or graphical procedures; however, the graphical approach involves extensive computation and a separate graphical integration for each point considered, and the analytical approach involves the approximation of the body shape by a suitable expression and (except in special cases) difficult and tedious integration.

Equation (1) may be written as

$$P_x = \sum_{i=1}^{i=n} \frac{2Q_i}{\sqrt{(x - \xi_i)^2 - (\beta R_x)^2}} \tag{3}$$

where each of the n point sources located on the axis of the body ahead of $(x - \beta R_x)$ represents a section of the body of length Δx. Comparison of equation (3) with equation (1) shows that

$$Q = f'(\xi)\Delta x \tag{4}$$

It is evident that, if the arbitrary body may be adequately represented by a relatively small number of point sources, the pressure distribution may be calculated rapidly by use of equation (3). The computation is greatly facilitated by the direct proportionality between the pressure coefficient and the value of Q for a single source. (See equation (3) for $n = 1$.) This direct proportionality allows the pressure field for a single source to be computed once as a function of βr and used for any source or sink at any Mach number within the limitations of the basic equations. This universal pressure field may be conveniently plotted as a "grid" of lines of constant pressure coefficient on the $x,\beta r$ plane. Values for this grid computed from equation (3) (for $n = 1$, $Q = 0.01$, $\xi = 0$; that is, a single source having a convenient value of Q and located at the origin of the grid) are presented as table I. The grid is plotted in figure 1. The pressure distribution over the body due to a single source representing any section of the body of length Δx may be readily obtained graphically by superimposing the origin of the grid at the source location on a drawing of the body shape (plotted as βR against x), and reading the pressure shown by the grid at a number of points on the body surface, and then multiplying these pressures by the ratio of the Q for the source being considered to the value of Q for which the grid was prepared. The process is repeated for each source necessary to represent the body, and the pressure coefficient at any point is obtained by adding the pressures at the point due to each source.

If the body is to be satisfactorily represented by a small number of discrete sources, the location of a source within its section of the

body will be important. It was found (see appendix) that the point source should be located on the axis $\Delta x/4$ ahead of the rear end of the section of the body of length Δx which it represented and the Q for the source should be computed from the radius and slope of the body surface at the source location. With this source location and strength, the pressures on the body surface at and behind the intersection of the Mach line from the axis at the end of the interval with the body surface closely approximated the pressures obtained from a continuous distribution of sources along the axis of the section. As the pressures on the body due to a number of sources are summed only at the intersection of the Mach line from the end of each interval with the body surface (see appendix), the infinite pressures which equation (3) gives for $x = \xi + \beta r$ (along the Mach line from each source) are avoided. The validity of results obtained by the point-source method and the computational procedures used are demonstrated by an example.

EXAMPLE

Computation of a pressure distribution by the point-source method is accomplished in the following steps:

(1) Divide selected body shape into sections and determine source locations.

(2) Graphically compute pressures on body due to sources of $Q = 0.01$ by successive superposition of grid on body shape plotted as βR against x.

(3) Prepare tabular form for recording values.

(4) Determine value of Q for each source.

(5) Compute pressure on body due to each source.

(6) Sum pressures due to each source to obtain desired pressure distribution.

A parabolic body of fineness ratio 12 was chosen for this example as representative of bodies suitable for treatment by the linearized theory and because it could be easily treated by the method of Jones and Margolis (reference 4) for comparison. The pressure distribution was computed at a Mach number of 1.41.

Body.- The body shape is specified by

$$R = \frac{1}{2F}(1 - 4x^2) \tag{5}$$

Equation (5) describes a parabolic body of unit length symmetrical about its maximum diameter which is located at $x = 0$. The body was arbitrarily

divided into 20 sections of equal length ($\Delta x = 0.05$), and, as described in the preceding section, a source location was chosen $\Delta x/4$ ahead of the end of each section.

Graphical computations.— The successive superposition of the grid origin at the chosen values of ξ is accomplished by plotting the grid and body shape to the same scale on separate sheets of semitransparent coordinate paper and matching the two sheets on a glass surface lighted from behind. A convenient size for the grid for most purposes has been found to be 10 by 15 inches with the βr–scale 10 times the x–scale. The grid (fig. 1) should be plotted carefully from the data of table I and can, of course, be used for all bodies and Mach numbers. The body shape (plotted in the form βR against x) is shown in figure 2 with the grid origin superimposed on the source $\xi = -0.2625$ which represents the section of the body between $x = -0.30$ and $x = -0.25$.

Table.— A convenient form for tabulating the values obtained in the computation is presented as table II. The abscissas of each of the 20 sources are arranged vertically in two sets on the left of the table and the values of P used for the grid are used for column headings. The values of x at which the lines of constant P of the grid cross the body surface are recorded in the appropriate column in the upper part of the table. For the case shown in figure 2 ($\xi = -0.2625$) the values of x in table II are underlined.

The last column in the upper part of table II, headed x_Σ, gives the values of x at which the pressures due to each source are to be summed. These values are obtained by superimposing the grid origin at the end of the interval and reading the value of x on the body where the line of $P = \infty$ (Mach line) crosses the body surface. For the interval just mentioned ($\xi = -0.2625$), the grid origin is set at $x = -0.25$ and the value found for x_Σ is -0.216.

Determination of Q for each source.— In this example the values of Q for each of the 20 sources may be found easily by use of equations (2), (4), and (5). In the more general case of the arbitrary body with which this paper is concerned, however, the value of Q for each source must be determined from the ordinates of the body by use of the differential forms of equations (2) and (4) as shown in figure 3. Any convenient increment may be used to determine the variation of $R(dR/dx)$ with x from the variation of R with x (lower part of fig. (3)). However, as the value of Q must be determined at the source location, $\Delta[R(dR/dx)]$ is taken from the midpoint to the end of the interval and multiplied by 2 (upper part of fig. 3). The ratios of the value of Q determined for each source to the value of Q used to prepare the grid (0.01) are tabulated in the last column of the lower part of table II opposite the value of ξ for each source.

Computation of pressures on body due to each source.— The data in the upper part of table II is the pressure distribution over the body if all

the sources have $Q = 0.01$. As the pressure at any point due to one source is directly proportional to the value of Q, the actual pressure distribution on the body due to the source is determined by multiplying the value of P heading each column by the ratio $\frac{Q_\xi}{Q_{grid}}$ for the particular source being considered. The resulting P is entered in the lower part of table II. For example, for the source $\xi = -0.2625$, the ratio $\frac{Q_\xi}{Q_{grid}}$ is -0.0118 and the pressure coefficient at $x = -0.210$ (upper part of table, line $\xi = -0.2625$, column $P = 0.5$) is $P = -0.0118(0.5) = -0.0059$ (lower part of table, line $\xi = -0.2625$, column $P = 0.5$). For the same source the pressure coefficient at $x = -0.132$ (upper part, line $\xi = -0.2625$, column $P = 0.16$) is $P = -0.0118(0.16) = -0.0019$ (lower part, line $\xi = -0.2625$, column $P = 0.16$). These values are bracketed in table II.

Summation of pressures due to each source.— The pressure coefficients for each source tabulated in the lower part of table II are plotted against the corresponding values of x at which they occur (upper part of table II) in figure 4. The logarithmic ordinate scale is used so that the points are separated at low values of the pressure coefficient. Curves are faired through the points for each source and all of the curves are added at the summation points previously determined (last column, upper part of table II). These sums and the values of x_Σ at which they occur are the desired pressure distribution on the body. The pressure coefficient at the nose of the body is computed directly from equation (A1) (see appendix) under the assumption that the extreme nose of the body approximates a cone.

Computation for different Mach numbers.— In order to compute the pressure distribution on the same body at a different Mach number, the body shape (in the form βR against x) must be replotted and the data in the upper half of table II redetermined. The data in the lower half of table II are not changed and the pressure distribution is computed from the new table exactly as in the preceding example.

Time required for computation.— Once the grid has been prepared, computation of a 20-point pressure distribution for an arbitrary body by this method required about 8 man-hours and, for the same body, results may be obtained for a different Mach number in about 4 additional man-hours. For parabolic bodies only the same number of points can be computed by the method of Jones and Margolis (reference 4) in somewhat less than half this time.

EVALUATION OF METHOD

Comparison with results by method of Jones and Margolis.— The pressure distribution determined in the example (fig. 4) is reproduced in figure 5 together with the pressure distribution computed for the same body by the method of Jones and Margolis (reference 4). The expression for this pressure distribution may be obtained from equations (1), (2), and (5) and is (see reference 4)

$$P_x = \frac{4}{F^2}\left\{\left[12x^2 - 1 + 6(\beta R_x)^2\right]\cosh^{-1}\left(\frac{x - x_o}{\beta R_x}\right) + 6\left[(x - x_o) - 4x\right]\sqrt{(x - x_o)^2 - (\beta R_x)^2}\right\} \tag{6}$$

Examination of figure 5 shows that the pressure distribution determined by the present method agrees with that of Jones and Margolis except for a small and apparently random scatter which approximately corresponds to the uncertainty of the graphical and numerical computations.

In order to investigate further the uncertainties introduced by the approximations involved in the point-source method, the pressure distribution was calculated for a parabolic body of fineness ratio 6. Inasmuch as large pressure coefficients and gradients are encountered for the body of fineness ratio 6 at $M = 1.41$, discrepancies should be more easily discernable than in the case of the body of fineness ratio 12. The results of this calculation for 10 and 20 intervals ($\Delta x = 0.10$ and 0.05) are compared in figure 6 with results calculated from equation (6). This fineness ratio was chosen because it approximates the lower limit of fineness ratio for which the linearized theory gives a completely supersonic flow field about the body at a Mach number of 1.41. It is interesting to note, however, that recent results obtained by the NACA wing-flow method showed that pressure distributions of the type predicted by Jones and Margolis occurred for a body of fineness ratio 6 at a much lower supersonic Mach number even though a large subsonic region was present at the nose.

Figure 6 shows that once more the results of the present method agree closely with those of Jones and Margolis. The scatter of the data in figure 6 (body of fineness ratio 6) appears to be somewhat greater than the scatter of the data in figure 5 (body of fineness ratio 12). Such a result might be expected because of the steeper gradients encountered on the body of fineness ratio 6. Little difference is evident in figure 6 between the results for the two different intervals.

As additional computations for the intervals of 0.02 (50 sections) near the nose of the body showed no significant difference from the results presented, it is concluded that the results obtained are not appreciably affected by the interval size (within the range investigated) and that a parabolic body may be satisfactorily represented by as few as 10 sources. The method does not require that a constant interval length be used and for arbitrary bodies it is recommended that shorter intervals be used in regions where the body cross section is changing rapidly.

The small discrepancies between the results computed by the point-source method and the method of reference 4 are negligible in comparison with the uncertainties introduced into both methods by the assumptions involved in the linear theory from which equations (1) and (2) are taken. The linear-theory results have been shown by several authors (for example, reference 2) to be in error by as much as 20 percent at some Mach numbers in the case of a 10° cone.

Comparison of results by point-source method with results by characteristics methods and with wind-tunnel measurements.- Some information on the usefulness and reliability of the point-source method may be obtained by comparison of results with results of calculations by the characteristics method and with wind-tunnel measurements for the German missile A4V1P presented in references 7 and 8. Pressure distributions measured at Mach numbers of 1.56 and 1.87 are presented in reference 7 and these measurements are compared with calculations by the graphical characteristics method of Tollmein and the computational characteristics method of Sauer in reference 8. The body shape of the A4V1P is not particularly suited for calculation by linearized methods because of the bluntness of the nose (ogival nose having a nose-length to maximum diameter ratio of 3.5, nose half angle 15.9°. However, the A4V1P is the only body for which relatively complete experimental data are available, and the comparison should indicate the accuracy with which the method predicts the pressure distribution on such relatively blunt bodies.

The measured pressure-distribution points and fairing (solid line) reproduced from reference 7 are shown in figure 7 together with the results obtained by the method presented herein (dash line). Examination of this figure shows that the point-source method satisfactorily reproduces the salient features of the measured pressure distribution but shifts the sharp breaks which occur at the beginning and end of the cylindrical section toward the rear of the body. The magnitude of the maximum positive and negative pressures are also somewhat exaggerated.

The fairing of the experimental data and the pressure distribution calculated by the point-source method shown in figure 7 are reproduced in figure 8 where they are compared with calculations by the characteristics methods of Sauer and Tollmein (reference 8). Figure 8 shows that Sauer's calculations agree closely with the experimental results and Tollmein's agree less closely, particularly near the middle of the nose and on the

cylindrical section of the body. The calculation by the point-source method agrees closely with that of Tollmein near the nose of the body, the most obvious discrepancy being the exaggeration and rearward shift of the minimum pressure peak near the beginning of the cylindrical section previously mentioned.

A comparison similar to that shown in figure 8 is presented in figure 9 for a Mach number of 1.56. In general, this comparison shows the same results as does figure 8; however, the overestimation of the pressures on the nose by the characteristics methods, which was barely visible in figure 8, is increased appreciably at the lower Mach number.

It will be noted that none of the calculated pressure distributions agree with the measurements on the rear ogive of the missile. Reference 7 states that the pressures in this region are greatly affected by the four large stabilizing tail fins which were in place when the measurements were made. Also, these pressures could be subject to large boundary-layer effects.

The sharp breaks in the pressure distributions for the A4V1P are characteristic of the class of bodies having cylindrical center sections faired into a curved nose and/or tail section so that the second derivative of the radius with respect to x is discontinuous. It is apparent, however, that the minimum pressure peak computed from equations (1) and (2) always occurs at a distance βR behind the beginning of the cylindrical section rather than at the beginning of the cylindrical section where the experimental results and rigorous theoretical treatment show it must be located. The occurrence of the rearward shift for one class of bodies suggests that such a shift may be present in the pressure-distribution results computed from equations (1) and (2) for other types of bodies. Extensive experimental pressure-distribution measurements are required to verify the existence of the shift for arbitrary bodies, however.

Inasmuch as the approximations involved in the linearized theory become more representative as the body becomes more slender and because, in general, slender bodies are better suited for aerodynamic purposes, the method presented herein is believed to provide a useful means for rapid estimation of the pressure distribution on slender, arbitrary bodies of revolution suitable for use as supersonic aircraft or missiles. Insufficient experimental evidence is available to establish definitely the limits of applicability of the method; however, it appears doubtful that results of usable accuracy could be obtained for bodies more blunt than the A4V1P used as an example herein.

Illustration of change in pressure distribution resulting from a moderate change in body shape.- In order to illustrate the magnitude of the changes in pressure distribution which result from moderate change in body shape the pressure distribution calculated for the test body of fineness ratio 12 used in the Langley Free-Fall Test Program is shown

in figure 10 compared with that for a parabolic body of the same fineness ratio. The body shapes are compared in the lower part of the figure. The free-fall test body was derived from an NACA low-drag airfoil and had a cusped tail faired into a tail boom and a relatively blunt nose.

Some indication of the over-all accuracy of the pressure distribution calculated for the free-fall test body may be obtained by comparison of the drag coefficient obtained by integrating the pressure distribution with the experimentally measured value. The computed value (0.080) is in good agreement with experimental results if a skin-friction coefficient of 0.003 based on surface area is assumed. Examination of figure 10 shows that the free-fall test body is more critical than the parabolic body with respect to flow separation because of the steep adverse gradient encountered near the rear of the body.

CONCLUDING REMARKS

A method is presented by which the pressure distribution on an arbitrary body of revolution moving at supersonic speeds may be calculated rapidly. The method was developed from the linearized potential-flow relations reported by Jones and Margolis in NACA TN No. 1081 and by other authors.

The method is essentially a graphical computing technique based on the assumption that a body may be represented satisfactorily by a relatively small number of point sources and sinks. Pressure distributions computed for parabolic bodies by this method were in excellent agreement with the results of Jones and Margolis. As few as 10 sources and sinks satisfactorily represented a parabolic body of fineness ratio 6.

Comparison of pressure distributions calculated for the German missile A4V1P with wind-tunnel measurements showed that the point-source method reproduced the salient features of the measured pressure distribution, but that the minimum pressure peak was exaggerated and shifted to the rear.

Pressure distributions for the A4V1P at Mach numbers of 1.87 and 1.56 computed by the point-source method were somewhat less satisfactory than those computed by the characteristics methods of Tollmein or Sauer. However, as the time required to compute a pressure distribution by the point-source method is appreciably less than is required by either of the two characteristics methods and as the salient features of the pressure distribution are satisfactorily reproduced, the point-source

method is believed to provide a useful means for rapid estimation of the pressure distribution on slender, arbitrary bodies of revolution suitable for supersonic aircraft or missiles.

Langley Aeronautical Laboratory
National Advisory Committee for Aeronautics
Langley Field, Va., September 23, 1948

APPENDIX

LOCATION OF A SINGLE SOURCE EQUIVALENT TO A CONTINUOUS DISTRIBUTION OF SOURCES WITHIN A FINITE INTERVAL

In the linearized theory of supersonic flows (references 1 to 5) bodies of revolution are assumed to be represented by a continuous distribution of sources and sinks along the axis of the body and the pressures resulting from these sources and sinks are assumed to be propagated only within the Mach cones. Thus, if an interval of length Δx extending from the vertex of a semi-infinite cone is considered, it is apparent that only at the intersection point (the intersection of the Mach cone from the axis at the end of the interval with the cone surface) is the pressure influenced by all of and only by that part of the continuous source distribution within the interval. As the rate of change of source strength $f'(\xi)$ is constant for a cone, the location of a single source which causes the same pressure at the intersection point as does the continuous distribution of sources within the interval may be determined in the following manner.

The pressure coefficient on the surface of a cone of semivertex angle θ due to a continuous distribution of sources along the axis may be found from equations (1) and (2) to be constant and equal to

$$P = 2\tan^2\theta \cosh^{-1}\left(\frac{\cot\theta}{\beta}\right) \tag{A1}$$

The pressure coefficient on the surface of the cone at any point x due to a single source located at ξ is (see equation (3) for $n = 1$)

$$P_x = \frac{2Q}{\sqrt{(x-\xi)^2 - (\beta R_x)^2}} \tag{A2}$$

As for the cone (with vertex at the origin)

$$R = x \tan\theta$$

then from equations (2) and (4)

$$Q = \Delta x \tan^2\theta$$

Equating the pressure coefficients given by equations (A1) and (A2) at the intersection point and expressing the location of the source ahead of the rear end of the interval as a fraction of the interval length $\left(\delta = \Delta x - \xi, \quad \tau = \frac{\cot \theta}{\beta}\right)$ gives

$$\frac{\delta}{\Delta x} = \frac{-1 + \sqrt{\left(\frac{\tau - 1}{\cosh^{-1} \tau}\right)^2 + 1}}{\tau - 1} \tag{A3}$$

Computations from equation (A3) for values of τ from 1.01 to 10.0 show that the ratio $\delta/\Delta x$ is approximately equal to 0.25. The maximum variation in this range, which corresponds to cone angles of 5° to 45° at $M = 1.41$ (or Mach numbers from 1.15 to 5.75 for a 10° cone), is less than ±1 percent of Δx.

An expression for the pressures on the surface of the cone behind the intersection point due to the continuous distribution of sources within the interval may be obtained from equation (1) by use of appropriate limits of integration. The variation of pressure with x given by this expression is closely approximated by equation (A2) for the source location just determined.

It is therefore evident that the pressure on the surface of a cone at and behind the intersection point due to a continuous distribution of sources along the axis within an interval Δx from the vertex is closely approximated by a single source located $\Delta x/4$ ahead of the end of the interval. Further computation along these lines has indicated that this principle may be applied to an interval located in any part of a conical or parabolic body of revolution with reasonable accuracy, provided that the pressure function Q is computed (equations (2) and (4)) from the radius and slope of the body surface at the source location. It appears reasonable to assume, therefore, that within the general limitations of the linear theory, the principle may be applied to arbitrary bodies.

REFERENCES

1. Von Kármán, Th.: The Problem of Resistance in Compressible Fluids. Volta Congress 1936, Reale Academia d'Italia, Rome.

2. Von Kármán, Theodore, and Moore, Norton B.: Resistance of Slender Bodies Moving with Supersonic Velocities, with Special Reference to Projectiles. Trans. A.S.M.E., vol. 54, no. 23, Dec. 15, 1932, pp. 303–310.

3. Lighthill, M. J.: Supersonic Flow past Bodies of Revolution. R. & M. No. 2003, British A.R.C., 1945.

4. Jones, Robert T., and Margolis, Kenneth: Flow over a Slender Body of Revolution at Supersonic Velocities. NACA TN No. 1081, 1946.

5. Sauer, Robert: Introduction to Theoretical Gas Dynamics. Springer–Verlag O. H. G., Berlin, 1943. (Translation by Hill and Alpher, J. W. Edwards Brothers, Ann Arbour, Michigan, 1947.)

6. Ferri, Antonio: Application of the Method of Characteristics to Supersonic Rotational Flow. NACA TN No. 1135, 1946.

7. Erdmann: Druckverteilungsmessung am A 4 V 1 P im Bereich der Unter– und Überschallgeschwindigkeiten. Archiv Nr. 66/100, Aerodynamisches Institut, Heeres Versuchsstelle, Peenemünde, Nov. 27, 1942.

8. Schubert, F.: The Axially Symmetric Flow about the A–4 for Mach Number 1.86 and 1.56. File Nr. 66/101, Institute of Aerodynamics, Army Experimental Station, Peenemünde, Nov. 17, 1942. (Translation)

TABLE I

VALUES FOR GRID (FIG. 1) OF LINES OF CONSTANT PRESSURE COEFFICIENT IN x,βr PLANE CALCULATED FROM EQUATION (3); SOURCE AT ORIGIN; PRESSURE FUNCTION Q = 0.01

P \ βr	0	0.01	0.02	0.03	0.05	0.09
	x					
∞	0	0.0100	0.0200	0.0300	0.0500	0.0900
2.00	.0100	.0141	.0224	.0316	.0510	.0908
1.00	.0200	.0224	.0283	.0361	.0538	.0922
.70	.0286	.0303	.0349	.0414	.0576	.0944
.50	.0400	.0412	.0447	.0500	.0640	.0995
.30	.0667	.0674	.0696	.0731	.0834	.1120
.20	.1000	.1005	.1020	.1044	.1118	.1345
.16	.1250	.1254	.1266	.1286	.1346	.1540
.10	.2000	.2002	.2010	.2022	.2062	.2193
.08	.2500	.2502	.2508	.2518	.2550	.2657
.05	.4000	.4001	.4005	.4011	.4031	.4100
.03	.6667	.6667	.6670	.6674	.6685	.6727
.02	1.0000	1.0000	1.0002	1.0004	1.0012	1.0040

TABLE II

FORM FOR TABULATING VALUES OF P ON SURFACE OF BODY DUE TO EACH SOURCE AND VALUES OF x AT WHICH THEY OCCUR. EXAMPLE: PARABOLIC BODY OF FINENESS RATIO 12 AT A MACH NUMBER OF 1.41

[Underlined and bracketed values are for example]

P / ξ	∞	1.0	[0.5]	0.3	0.2	[0.16]	0.10	0.08	0.05	0.03	x_Σ
	x										
-0.4625	-0.455	-0.441	-0.421	-0.394	-0.361	-0.335	-0.260	-0.211	-0.062	0.204	-0.441
-.4125	-.397	-.386	-.368	-.342	-.309	-.284	-.210	-.160	-.010	.255	-.383
-.3625	-.340	-.331	-.315	-.290	-.258	-.233	-.159	-.110	.040	.305	-.326
-.3125	-.284	-.277	-.264	-.238	-.208	-.183	-.110	-.060	.090	.355	-.270
-.2625	-.230	-.225	-.210	-.188	-.156	-.132	-.060	-.010	.140	.405	-.216
-.2125	-.175	-.171	-.159	-.135	-.105	-.081	-.009	.041	.190	.455	-.162
-.1625	-.124	-.119	-.107	-.085	-.055	-.030	.040	.090	.240	-----	-.110
-.1125	-.071	-.068	-.056	-.034	-.005	.019	.090	.140	.288	-----	-.059
-.0625	-.020	-.016	-.005	.017	.046	.070	.141	.190	.339	-----	-.008
-.0125	.027	.031	.042	.064	.094	.116	.188	.237	.386	-----	.041
.0375	.078	.082	.093	.115	.144	.167	.240	.289	.436	-----	.090
.0875	.126	.130	.141	.164	.193	.217	.289	.338	.488	-----	.139
.1375	.175	.179	.190	.213	.243	.266	.338	.388	-----	-----	.186
.1875	.221	.225	.238	.261	.290	.315	.387	.436	-----	-----	.233
.2375	.267	.274	.285	.309	.339	.363	.436	.487	-----	-----	.280
.2875	.314	.320	.334	.356	.390	.414	.492	-----	-----	-----	.325
.3375	.358	.365	.381	.405	.438	.464	-----	-----	-----	-----	.370
.3875	.403	.412	.430	.455	.488	-----	-----	-----	-----	-----	.415
.4375	.445	.460	.478	-----	-----	-----	-----	-----	-----	-----	.456
.4875	.490	-----	-----	-----	-----	-----	-----	-----	-----	-----	-----
ξ	P										$\frac{q_\xi}{q_{grid}} = 100q_\xi$
-0.4625	∞	0.1085	0.0542	0.0326	0.0217	0.0174	0.0108	0.0087	0.0054	0.0033	0.1085
-.4125	∞	.0725	.0362	.0218	.0145	.0116	.0073	.0058	.0036	.0022	.0725
-.3625	∞	.0398	.0199	.0119	.0080	.0064	.0040	.0032	.0020	.0012	.0398
-.3125	∞	.0112	.0056	.0034	.0022	.0018	.0011	.0009	.0006	.0003	.0112
[-.2625]	∞	-.0118	[-.0059]	-.0035	-.0024	[-.0019]	-.0012	-.0009	-.0006	-.0004	[-.0118]
-.2125	∞	-.0315	-.0158	-.0094	-.0063	-.0050	-.0032	-.0025	-.0016	-.0009	-.0315
-.1625	∞	-.0475	-.0238	-.0142	-.0095	-.0076	-.0048	-.0038	-.0024	------	-.0475
-.1125	∞	-.0594	-.0297	-.0178	-.0119	-.0095	-.0059	-.0048	-.0030	------	-.0594
-.0625	∞	-.0660	-.0330	-.0198	-.0132	-.0106	-.0066	-.0053	-.0033	------	-.0660
-.0125	∞	-.0692	-.0346	-.0208	-.0138	-.0111	-.0069	-.0055	-.0035	------	-.0692
.0375	∞	-.0683	-.0342	-.0205	-.0137	-.0109	-.0068	-.0055	-.0034	------	-.0683
.0875	∞	-.0633	-.0316	-.0190	-.0127	-.0101	-.0063	-.0051	-.0032	------	-.0633
.1375	∞	-.0537	-.0268	-.0161	-.0107	-.0086	-.0054	-.0043	------	------	-.0537
.1875	∞	-.0403	-.0202	-.0121	-.0081	-.0064	-.0040	-.0032	------	------	-.0403
.2375	∞	-.0222	-.0111	-.0067	-.0044	-.0036	-.0022	-.0018	------	------	-.0222
.2875	∞	0	0	0	0	0	0	------	------	------	0
.3375	∞	.0255	.0128	.0077	.0051	.0041	------	------	------	------	.0255
.3875	∞	.0553	.0276	.0166	.0111	------	------	------	------	------	.0553
.4375	∞	.0900	.0450	------	------	------	------	------	------	------	.0900
.4875	∞	.1290	------	------	------	------	------	------	------	------	.1290

NACA

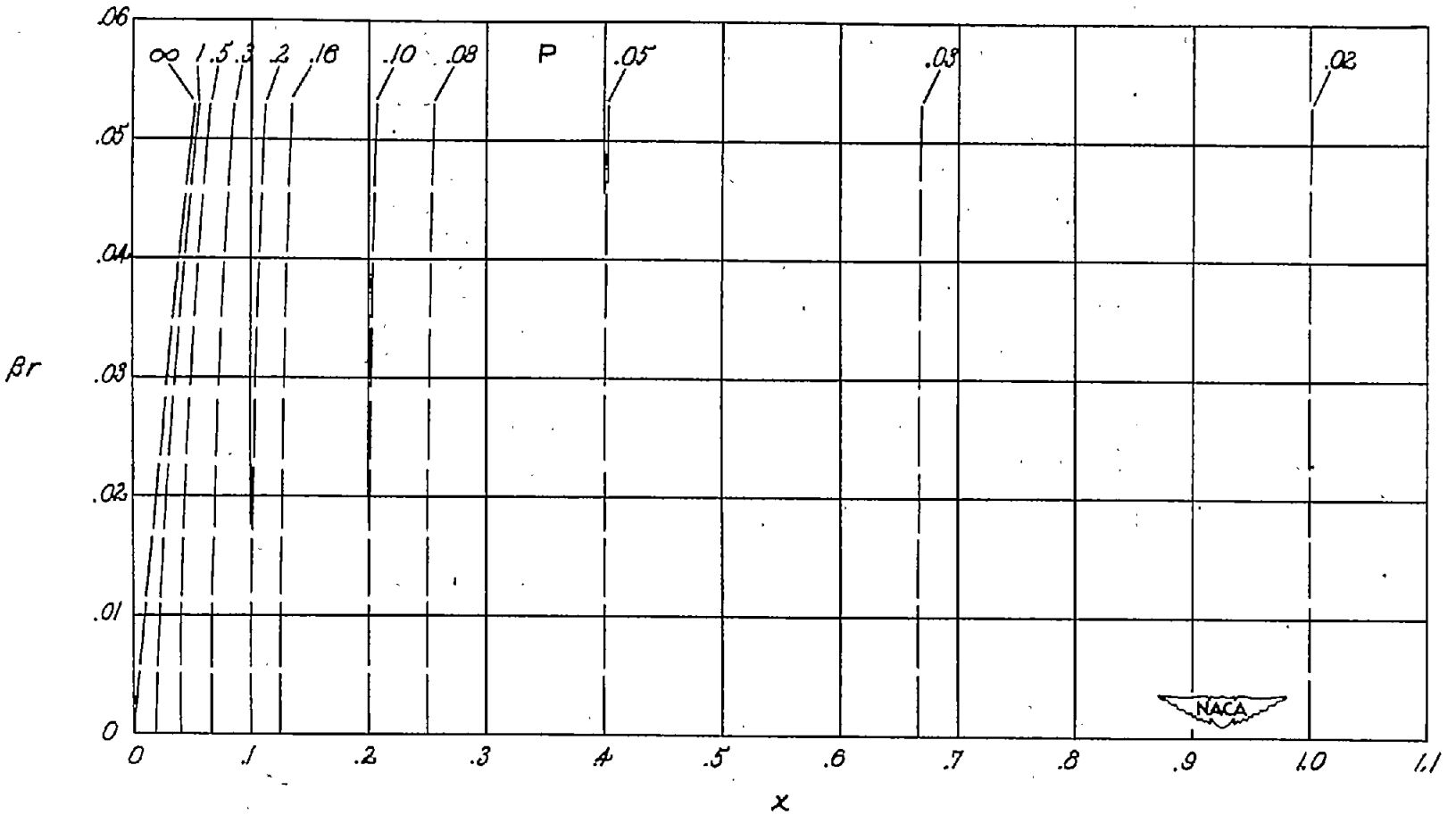

Figure 1.- Grid of lines of constant pressure coefficient P for supersonic source of Q = 0.01 plotted on x,βr plane. Ordinate scale is 10 times abscissa scale.

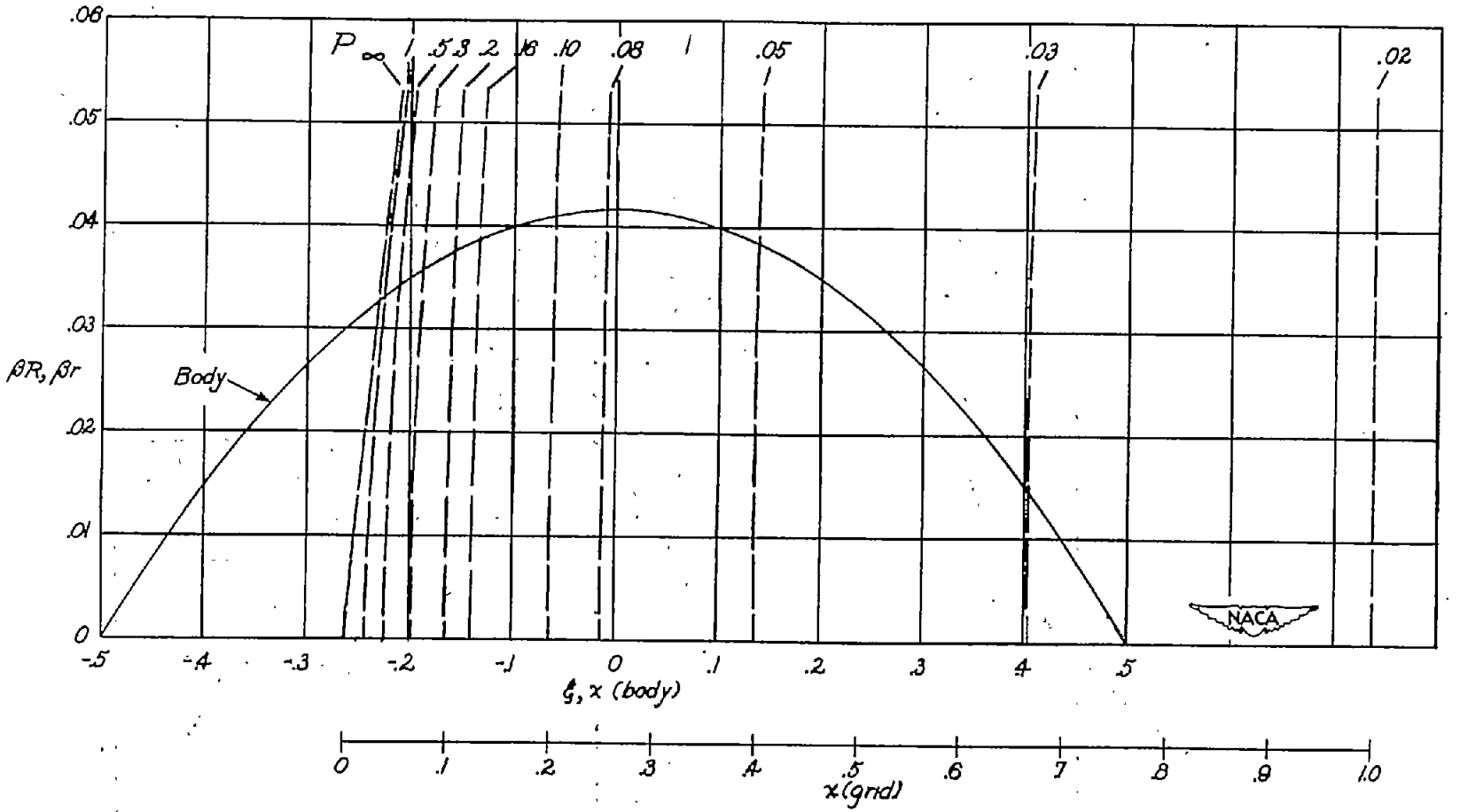

Figure 2.- Parabolic body of fineness ratio 12 plotted on x,βr plane for M = 1.41. Grid (fig. 1) is shown superimposed on body with origin of grid located at source location ξ = -0.2625. Ordinate scale is 10 times abscissa scale.

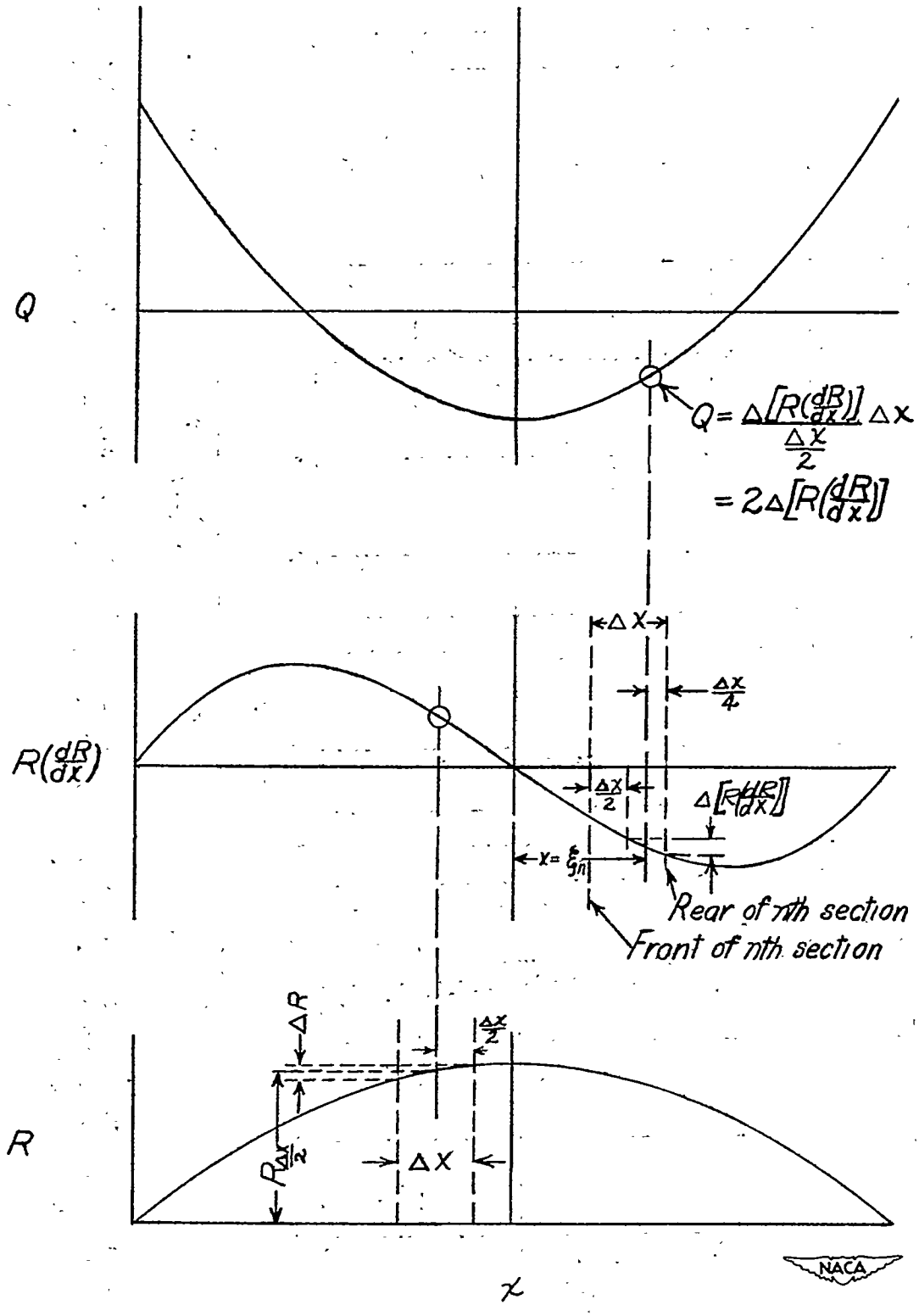

Figure 3.- Method of obtaining Q for arbitrary bodies.

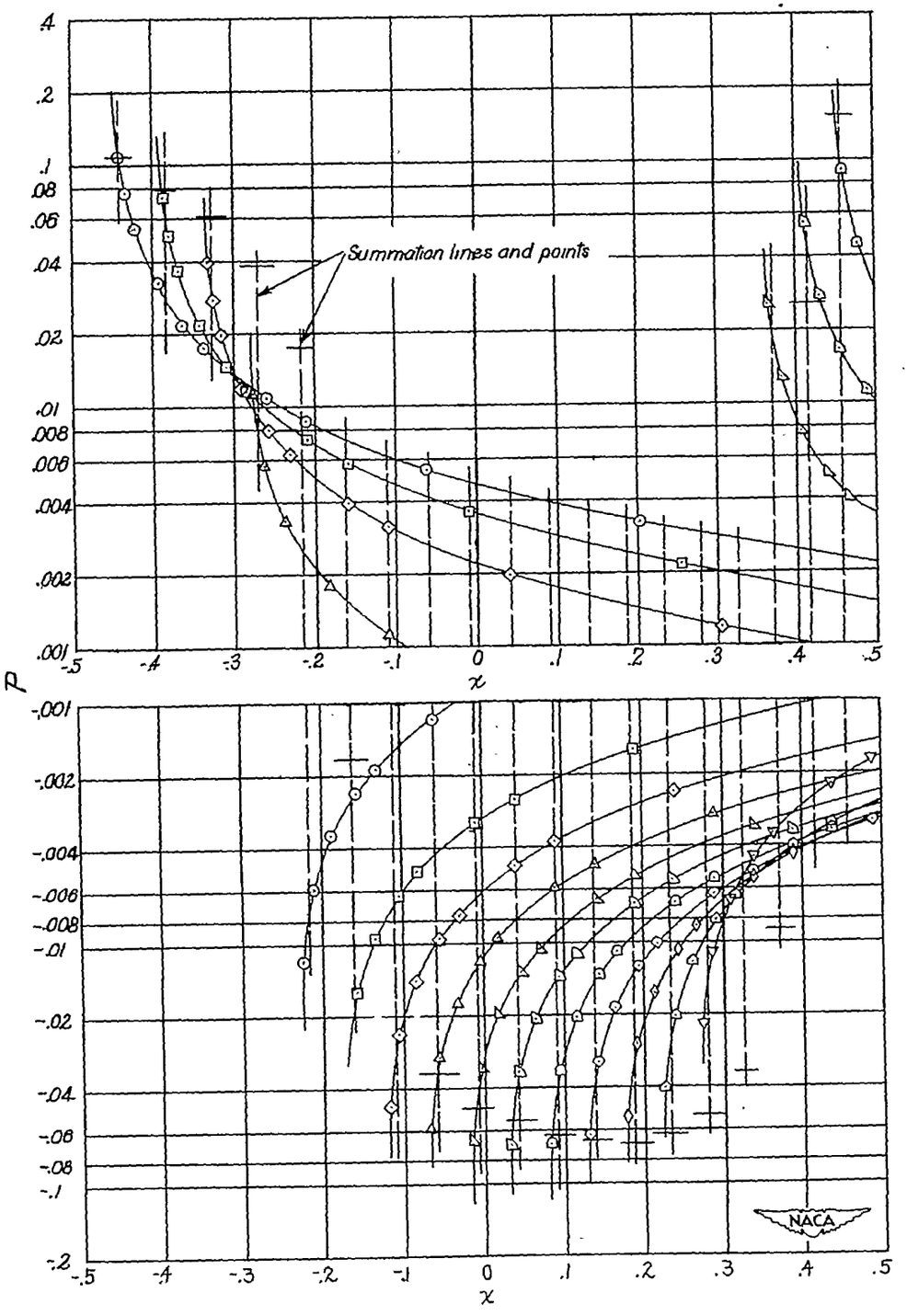

Figure 4.- Variation of pressure coefficient P along the surface of the parabolic body of fineness ratio 12 due to each source (see table II) at a Mach number of 1.41.

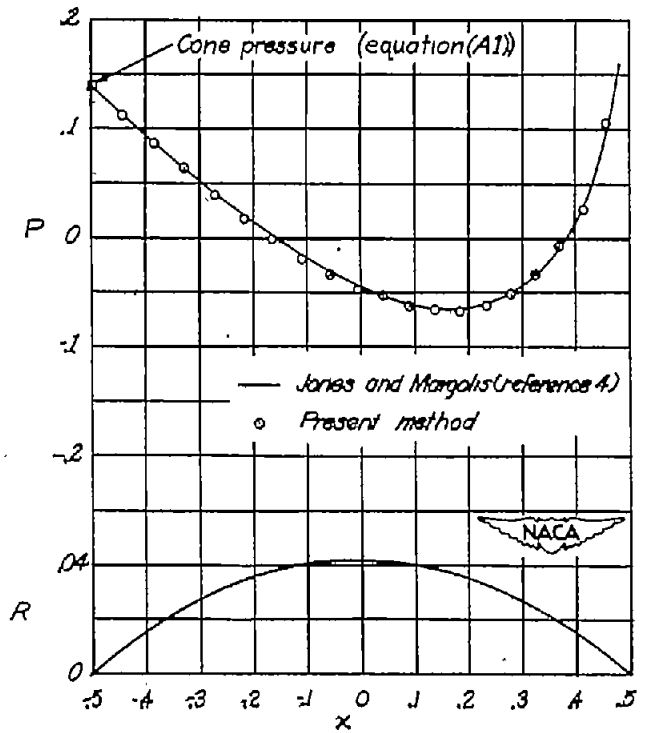

Figure 5.- Comparison of pressure distributions for a parabolic body of fineness ratio 12 computed at a Mach number of 1.41 by the point-source method and by the method of Jones and Margolis (reference 4).

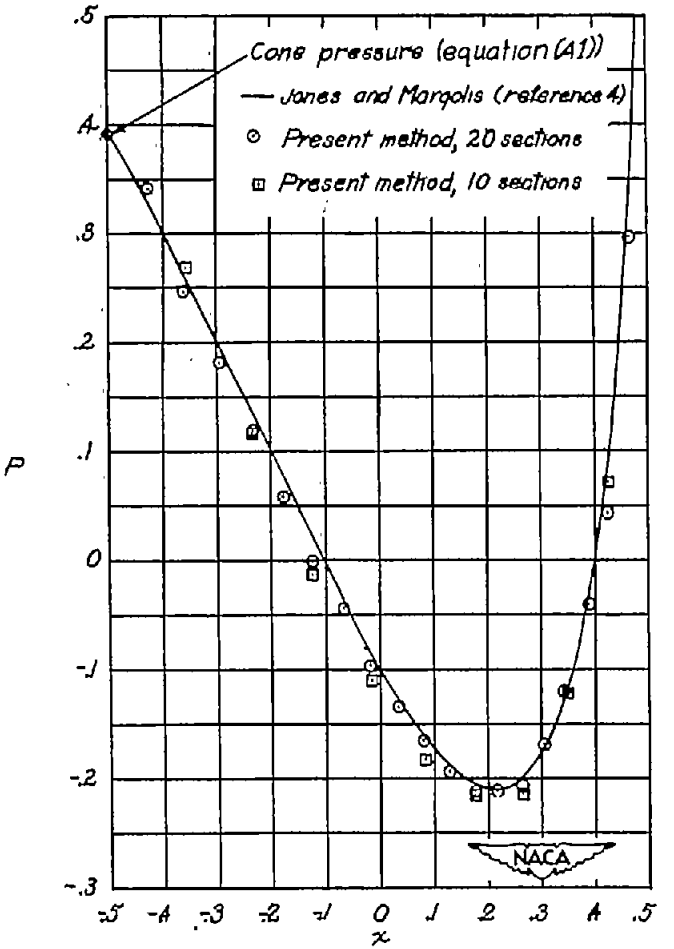

Figure 6.- Comparison of pressure distributions for a parabolic body of fineness ratio 6 computed at a Mach number of 1.41 by the point-source method and by the method of Jones and Margolis (reference 4).

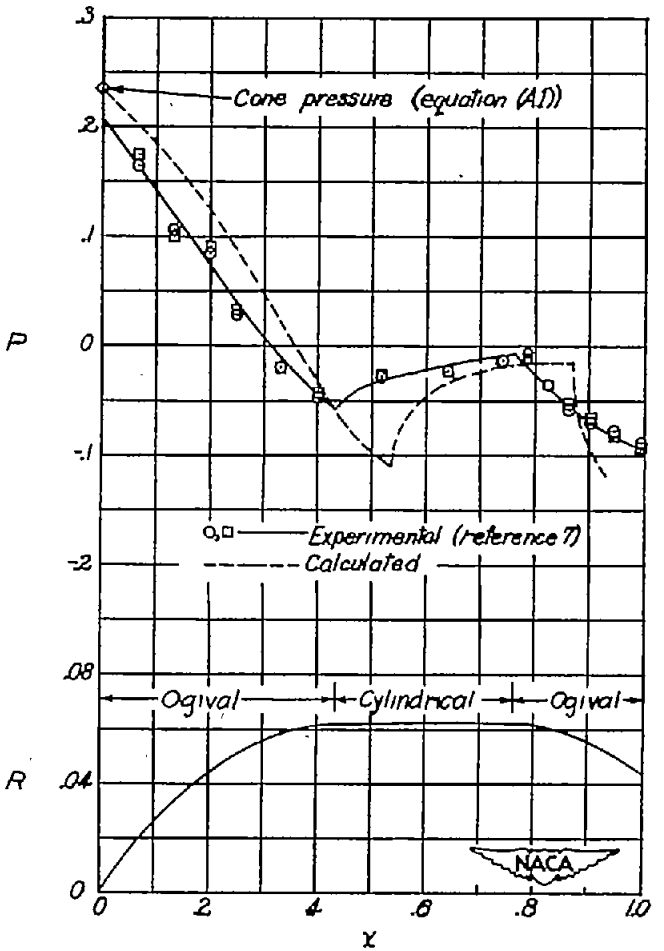

Figure 7.- Comparison of calculated and experimental pressure distributions for the A4V1P at a Mach number of 1.87. Experimental points and solid fairing taken from reference 7.

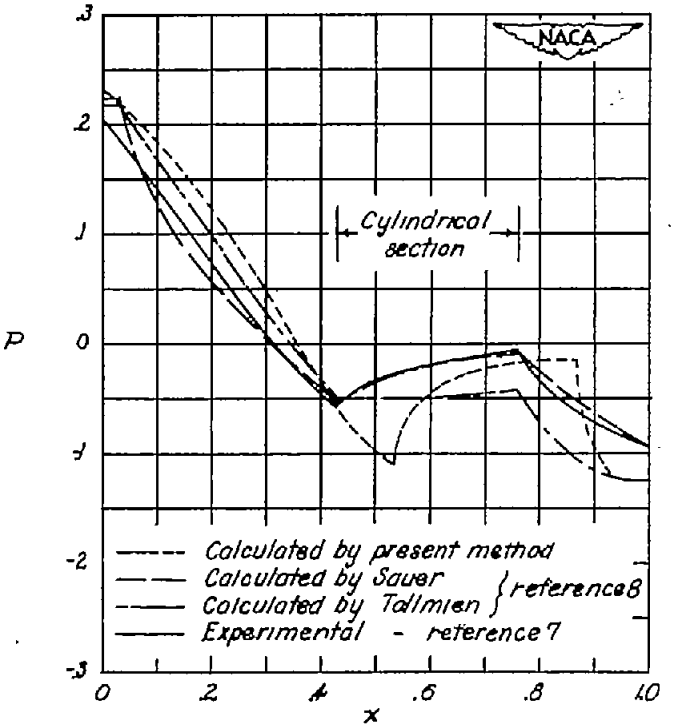

Figure 8.- Comparison of pressure distributions calculated by the present method and by the characteristics methods of Sauer and Tollmein with wind-tunnel results for the A4V1P at a Mach number of 1.87.

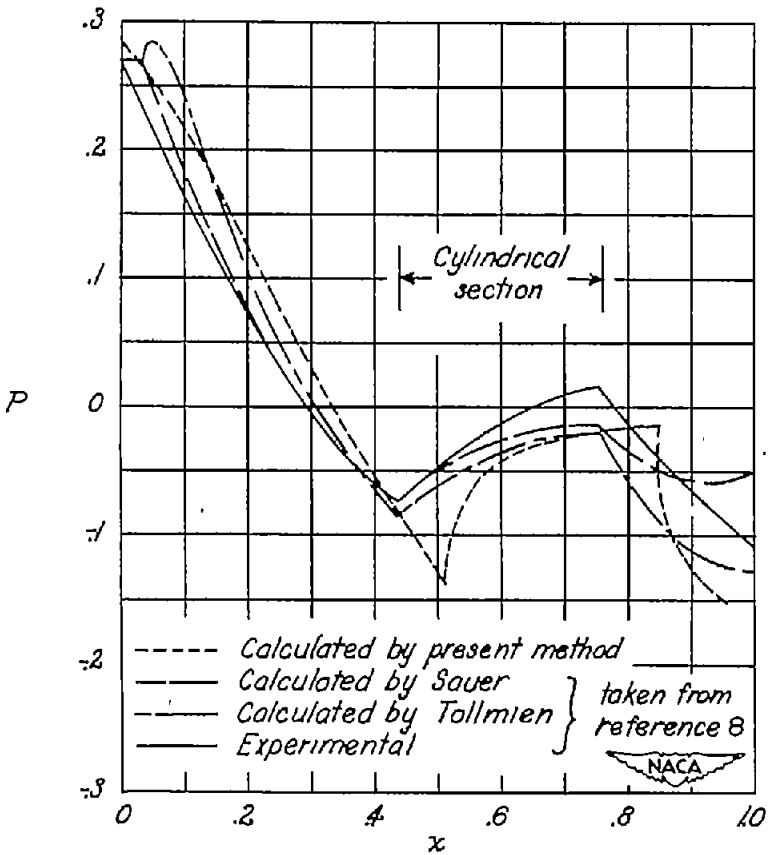

Figure 9.- Comparison of pressure distributions calculated by the present method and by the characteristics methods of Sauer and Tollmein with wind-tunnel results for the A4V1P at a Mach number of 1.56.

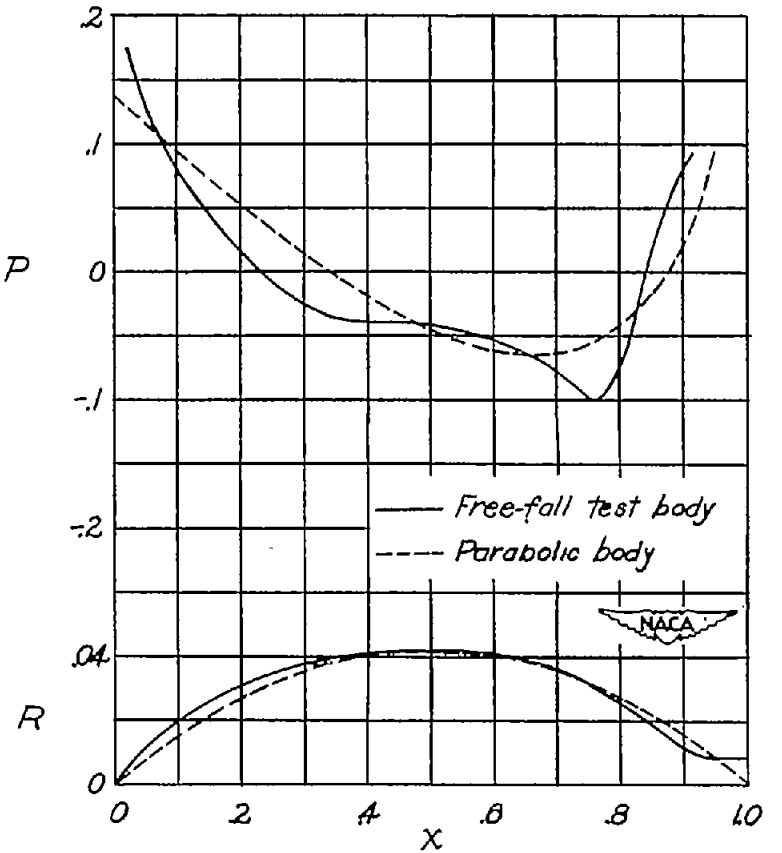

Figure 10.- Comparison of pressure distributions calculated at a Mach number of 1.41 by the point-source method for a parabolic body of fineness ratio 12 and for the free-fall test body of fineness ratio 12.